Investigation of Performance-Enhanced ROADMs for N-WDM Superchannels Carrying High-Order QAM

Chen Zhu[1], Bill Corcoran[1,2], Leimeng Zhuang[1], Jochen Schröder[2,3], Marizio Burla[4], Willem P. Beeker[5], Arne Leinse[5], Chris G.H. Roeloffzen[6], and Arthur J. Lowery[1,2]

[1]*Electro-Photonics Laboratory, Dep. Elec and Comp. Syst. Eng., Monash University, VIC 3800, Australia*
[2]*Centre for Ultrahigh-bandwidth Devices for Optical Systems (CUDOS), Australia*
[3]*School of Electronic and Computer Systems Engineering, RMIT University, Melbourne, Australia*
[4]*Institut National de la Recherche Scientifique (INRS-EMT), Montréal, Canada*
[5]*LioniX BV, PO Box 456, Enschede, 7500 AL, the Netherlands*
[6]*SATRAX BV, PO Box 456, Enschede, 7500 AL, the Netherlands*
Email: chen.zhu@monash.edu

Abstract: Adding a ring-resonator-assisted MZI for preprocessing improves the selectivity of ROADMs, enabling cascades of ROADMs to process N-WDM superchannels. We experimentally investigate the N-WDM superchannels performance with high-order QAM after filtered by cascaded enhanced ROADMs.

OCIS codes: (060.1660) Coherent communications; (120.2440) Filter; (060.4230) Multiplexing.

1. Introduction

Nyquist filtering provides an inter-symbol-interference (ISI) free impulse response to rectangularly shape each channel, which allows packing multiple channels at close-to-symbol-rate channel spacing, without impaired by inter-channel-interference (ICI) [1]. After transmission, with powerful digital signal processing (DSP) to remove the channel and subsystem impairments, the system performance is ideally limited by the amplified spontaneous emission (ASE) noise and fiber nonlinear interference. However, considering a practical dynamic optical routing network that consists of many reconfigurable optical add-drop multiplexer (ROADM) nodes, the non-idea ROADM filtering induced-ICI can become a major factor for the trade-off between achievable reach and channel spacing.

As the transition band roll-off of the commercial liquid crystal on silicon based wavelength selective switch (LCoS-WSS) is limited by the filter spectral resolution to approximately ten GHz, several schemes have been proposed to enhance the WSS resolution [2-4]. In [2], using an array waveguide grating as the spectral disperser preceding of LCoS-WSS has been reported to realize 0.8-GHz filtering resolution; and a delay-line based optical finite-impulse-response (FIR) filter is reported to support channel filtering in a N-WDM superchannel with 37.5-GHz channel spacing and 15% guard band [3]. More recently, we have demonstrated a Nyquist ROADM that employed a two-ring-resonator-assisted Mach-Zehnder interferometer (2RAMZI) with 8% roll-off to de-interleave the even and odd N-WDM channels, which allows the subsequent LCoS-WSSs to switch the N-WDM channels [4].

Since all the above mentioned demonstrations are limited to QPSK format with fixed guard band and passing through only a single ROADM node, it may not be very indicative for practical N-WDM system design. In this work, we present a systematic experimental investigation of the N-WDM system tolerance in the presence of accumulated enhanced WSS filtering induced ICI, with high-order QAM modulation formats and different guard bands. 8/16/32/64-QAM N-WDM superchannel with 4%, 8%, 20% and 50% guard bands have been filtered by the EWSS multiple times, to test the number of ROADM nodes that different systems can reach.

2. Experimental setup

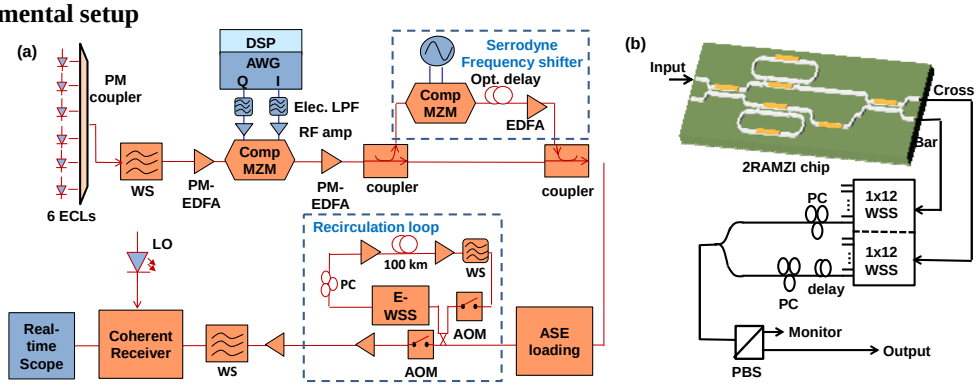

Fig. 1. (a) Experimental setup, (b) structure of the performance-enhanced ROADM.

The experimental setup is shown in Fig. 1(a). The transmitter comprised of 6 external cavity lasers (ECLs), spaced at 25 GHz, power equalized by a Finisar Waveshaper (WS), and then modulated by electrical signals generated from an Agilent 64 GSa/s DAC. The baseband signals were first modulated with 8/16/32/64 QAM formats, and then pulse shaped by a 0.01 roll-off root-raised-cosine (RRC) filter, with subsequent pre-emphasis to compensate the DAC and modulator responses. The per-channel symbol rate was set to 12, 11.6, 10 and 8.25 Gbaud, corresponding to 4%, 8%, 20% and 34% guard band ratios, respectively. The 6 modulated channels were equally split into two arms, with one arm delayed and frequency shifted by 12.5-GHz before recombining with the through arm, to form a superchannel. The optical spectrum measured with a 15-MHz resolution spectrometer (Agilent 83453B), of the combined superchannel with 4% guard band ratio is shown as Fig. 2(a).

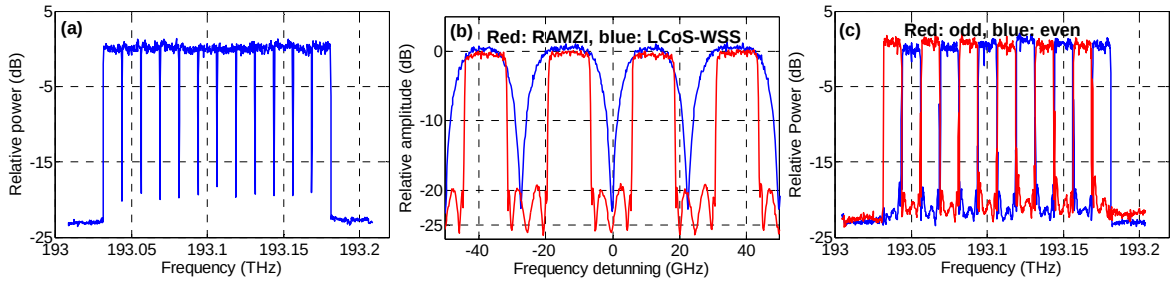

Fig. 2.: Measured spectra of: (a) WSS and RAMZI at cross port, (b) transmitted superchannel, (c) filtered odd and even channels.

The signals were then launched into a recirculating loop, consisting of two acousto-optic modulators (AOM), one 100-km span of standard single mode fiber, an EWSS for ROADM emulation, a WS for gain flattening and several erbium doped fiber amplifiers (EDFAs). As shown in Fig. 1(b), the EWSS setup is similar to that in [4], first employing a 2RAMZI circuit with 12.5 GHz free spectral range to interleave the odd and even superchannels into cross and bar port outputs, respectively. Two 1×12 LCoS-WSSs were then used to route the superchannel. In this demonstration, the WSSs were set to pass all the even/odd channels that processed. The measured responses of the 2RAMZI and LCoS-WSS for the cross port are shown in Fig. 2(b), note that the LCoS-WSS suppress part of the 2RAMZI induced ICI. The odd and even channels after the EWSS were then recombined with a 3-dB optical coupler, with the even channels delayed by ≈10 ns to de-correlate the signals and inter-channel cross-talk. As such, each channel experiences similar ICI, which is accumulated loop by loop. The odd and even channels' spectra after EWSS before recombining are shown in Fig. 2(c). Since the 2RAMZI only supports single polarization, we used two polarization controllers (PC) and a polarization beam splitter (PBS) to align the cross and bar port outputs. We also used one PC to compensate for the loop fiber's polarization rotation, which was necessary to guarantee the signal's polarization aligned with EWSS every loop. The polarization control would not be needed with a polarization-diverse 2RAMZI circuit for dual-polarization signals. At the receiver, another WS was used to select the channel of interest for coherent detection and sampling. The offline DSP include resampling to 2-Sa/symbol, matched filtering, dual stage adaptive equalization and maximum likelyhood based carrier recovery [5].

3. Experimental results

Figure 3(a) compares the 12-Gbaud signal OSNR performance of back-to-back transmission with that passing through one loop. The Q^2 results (Q^2(dB)=20log$_{10}$[$\sqrt{2}$efrc^{-1}(2BER)]) show that the required OSNR penalties at 7% FEC threshold (BER=3.8×10^{-3}) for 8-QAM, 16-QAM and 32-QAM are 1-dB, 4-dB and 7-dB, respectively. With 20% FEC threshold (BER=0.027 [6]), the OSNR penalty becomes 0.7-dB, 1.2-dB and 2-dB for 8-QAM, 16-QAM and 32-QAM, respectively. The 64-QAM signal with only 500-MHz guard band is not able to reach the 20% FEC threshold. All modulation formats suffer similar ICI due to non-idea EWSS filtering. To explain the increased OSNR penalty for higher-order modulation formats, we should first note that for our setup, the achievable system SNR (namely reference-SNR) without noise loading is about 20-dB (mainly limited by the achievable extinction of the serrodyne frequency shifter, electronic background noise and subsystem imperfections), and for a practical system the reference-SNR is normally under 25-dB. So the optical noise dominates the system performance with OSNR much less than the reference-SNR (e.g. 15-dB in this scenario), where the Q^2 factor is almost 1dB/dB relationship with the OSNR; while with increased OSNR that larger than 15-dB, the optical noise has less impact on the receiver SNR which determines the detection error. In other words, when operating in the region where OSNR is much higher than the reference-SNR, we expect less than 1-dB SNR improvement for a 1-dB increase in OSNR. For a higher-order modulation format to achieve a certain BER level, it must be operated in much higher OSNR region than for lower-order modulation formats, which translates to much larger required OSNR margin in the presence of ICI. So for high-order QAM transmission in the presence of ICI, the required OSNR margin can be reduced effectively by using larger FEC overheads that allows the system to be operated in a lower OSNR region.

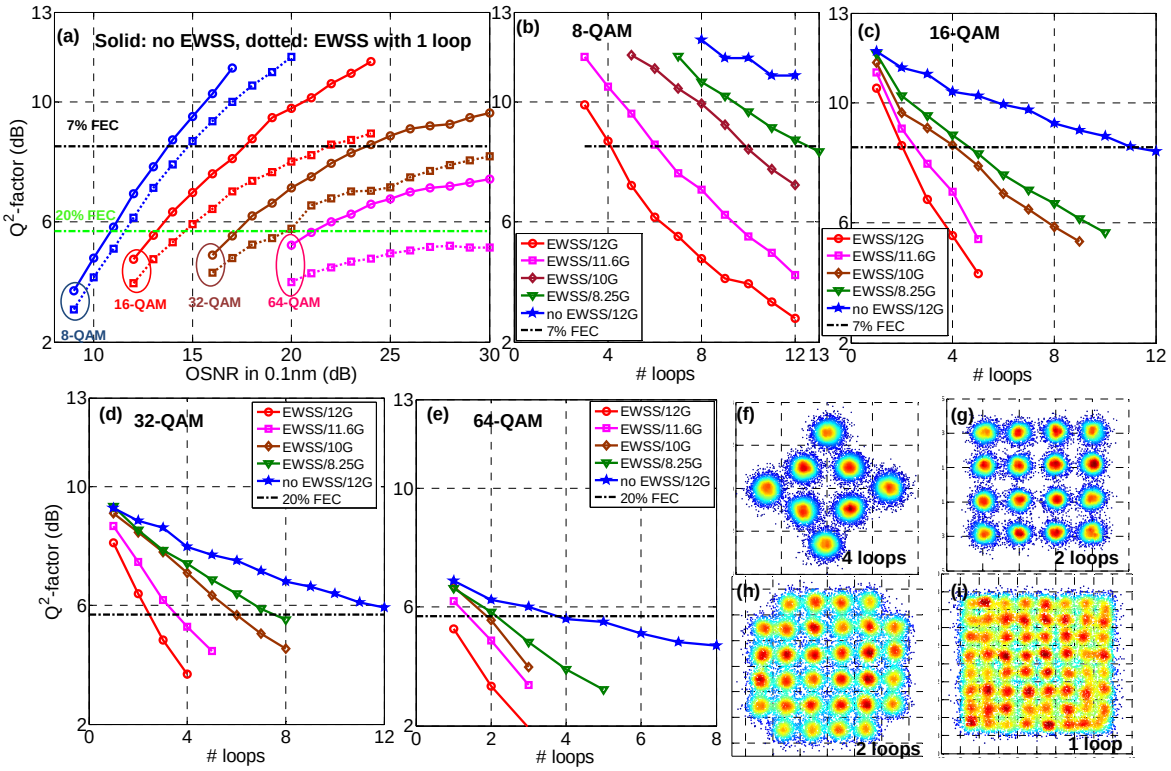

Fig. 3.: (a) OSNR measurements, (b)-(e): results with different number of loops for different modulation formats with different guard bands, (f)-(i) equalized constellation diagrams for different modulation formats.

Figures 3(c)-(e) depict the system performance over multiple loops. With 4% guard band ratio, 12-Gbaud 8-QAM and 16-QAM are able to transmit 4 and 2 loops with 7% FEC, respectively, which can be improved to 6 and 3 loops, by reducing the channel symbol rate to 11.6 Gbaud; with 20% FEC, 32-QAM is able to tolerant the accumulated ICI from 2 ROADM nodes and 64-QAM is not able to transmit over a single ROADM node, which can be improved to 6 and 2 ROADM nodes for 32-QAM and 64-QAM, by increasing the guard band ratio to 20%. Compared with the system with no EWSS in the recirculation loop, even 50% guard band system has certain penalty, which we attribute to the EWSS insertion losses (~20dB). The equalized signal constellations for 12-Gbaud system after multiple loops transmission are depicted in Figs. 3(f)-(i), for 8/16/32/64-QAM modulation formats.

4. Conclusion

We investigate the N-WDM superchannel system tolerance to wavelength switching with an performance-enhanced ROADM consisting of a 2RAMZI interleaver followed by off-the-shelf LCoS-WSSs. With only 4% guard band, 8-QAM and 16-QAM systems are able to tolerant 4 and 2 times ROADM filtering at 7% FEC threshold, while 32-QAM is able to transmit over 2 ROADM nodes with 20% FEC, while 64-QAM can only manage to pass one ROADM node with the gaud band ratio is increased to 20%.

Acknowledgement
This work is supported by the Australian Research Council's grants FL13010041 & CE110001018.

[1] G. Bosco, *et al*., "On the performance of Nyquist-WDM terabit superchannels based on PM-BPSK, PM-QPSK, PM-8QAM or PM-16QAM subcarriers," J. Lightwave Technol., **29**, 53-61 (2011).
[2] R. Rudnick, *et al*., "Sub-banded / single-sub-carrier drop-demux and flexible spectral shaping with a fine resolution photonic processor" in Proc. ECOC, PD.4.1, Cannes (2014).
[3] T. Goh, *et al*., "Optical Nyquist-filtering multi/ demultiplexer with PLC for 1-Tb/s class super-channel transceiver" in Proc. OFC, Tu3A.5, L.A. (2015).
[4] B. Corcoran, *et al*., "A wavelength selective switch for optical add/drop multiplexing of sub-bands within Nyquist WDM super-channels," in Proc. ECOC 2015, Valencia, paper Tu.3.5.2.
[5] C. Zhu, *et al*., " Frequency-domain blind equalization for long-haul coherent Pol-Mux 16-QAM system with CD prediction and dual-mode adaptive algorithm," IEEE Photonics Journal, 4, 1653-1661, (2012).
[6] D. Chang, *et al*., "LDPC convolutional codes using layered decoding algorithm for high speed coherent optical transmission" in Proc. OFC, OW1H. 4, L.A. (2012).